Available online at www.sciencedirect.com

SciVerse ScienceDirect

Energy Procedia 37 (2013) 5562 – 5569

Energy Procedia

GHGT-11

Simulation study of density-driven natural convection mechanism in isotropic and anisotropic brine aquifers using a black oil reservoir simulator

Amir Taheri[a,]*, Dag Wessel-Berg[b], Ole Torsæter[a]

[a]*NTNU, Departement of Petroleum Engineering and Applied Geophysics, S.P. Andersens Vei 15a, 7491 Trondheim, Norway*
[b]*Sintef Petroleum Research, S.P. Andersens Vei 15b, N-7465 Trondheim, Norway*

Abstract

For simulation models of density-driven natural convection in brine aquifers gravitational instabilities are usually triggered by numerical round off errors. Using this method for initiating onset of convective flow, simulation results show that the onset time for convection is orders of magnitude larger than the ones predicted by theoretical stability analysis theory.
In this study, a new approach for initializing of the model is developed based on available theoretical works. This initialization method is seen to give more accurate predictions of onset time for convection in the simulation models of isotropic and anisotropic brine aquifers.

Keywords: brine aquifers; convection; critical time; initializing; perturbation; isotropic; anisotropic

1. Introduction

CO_2 storage into saline brine aquifers are considered as one of the most favorable options for decreasing the emissions of CO_2 to the atmosphere. In this setting CO_2 dissolution is regarded as a medium to long scale trapping mechanism of CO_2. Dissolved CO_2 in brine increases the density of the brine-CO_2 solution, and the initiation of gravitational instability leads to density-driven natural convection increasing the dissolution rate of free CO_2 into the brine. Density driven convection occurs when the Rayleigh number $R_a = (\Delta\rho g k_v H)/(\varphi\mu D)$ (corresponding to dimensionless depth of the aquifer) is larger than approximately 40 [1]. $\Delta\rho$, g, H, k_v, φ, μ and D are mass density increase for fully CO_2 saturated brine, acceleration of gravity, thickness, absolute vertical permeability, porosity, brine viscosity and diffusivity

* Corresponding author. Tel.: +47-735-95105; fax: +47-739-44472.
E-mail address: amir.taheri@ntnu.no.

doi:10.1016/j.egypro.2013.06.477

respectively. The correct estimation of the onset time for convection and the rate of dissolution are important because the timescale for dissolution corresponds to the timescale over which free phase CO_2 has a chance to leak out.

For simulation of density-driven natural convection mechanism in brine aquifers the system is usually initialized with a free phase CO_2 below the cap rock and above the brine. The instability is triggered by numerical round off errors in the finite difference flow simulations. With this approach for simulation, the results show that the onset time for convection is orders of magnitude larger than the ones predicted by stability analysis theory. Also the minimum Rayleigh number for initiation of instability and convective mixing in numerical reservoir simulation is significantly larger than the reported value of 40. These differences will be more highlighted by decreasing the aquifer permeability [2, 3].

In this study, we are going to perform some numerical simulation studies using a black oil simulator with a new approach for initializing of the brine aquifer models and for more accurate estimation of onset time for instability. This new initializing approach is derived from the theoretical analyses that will be addressed in the next section [4]. This method is examined for brine aquifers with isotropic and anisotropic permeability and enough sensitivity is performed on system properties.

2. Theoretical analyses related to onset time for convection

In this paper we use the results from Wessel-Berg [4] on the linearized analysis of gravitational instability of a diffusive boundary layer in a semi-infinite anisotropic homogeneous brine aquifer. For finite depth aquifers, the magnitude of the Rayleigh number indicates the presence or not of the considered instability.

In this study, Darcy's and Fick's law are considered in the governing equations, and the CO_2 source for the model is implemented as a boundary condition by putting the CO_2 concentrations to its maximum at the top of the aquifer. The two unknown functions in this problem are the CO_2 concentration C(x,y,z,t) and the pressure p(x,y,z,t). The scaling numbers used in this study are $L = (\varphi\mu D)/(\Delta\rho g k_v)$ as the length scale and $T = L^2/D$ as the time scale for scaling the physical lengths and times to dimensionless ones.

Considering erfc(x) as the complementary error function, and z and t as dimensionless depth below the top boundary and dimensionless time, $C^B(z,t) = \mathrm{erfc}(z/2\sqrt{t})$ and $p^B(z,t) = \int_0^z C^B(u,t)du$ are considered as the basic solutions for the dimensionless boundary value problem. This basic solution describes a pure diffusion process without convection flow. For describing the convection flow, the perturbations away from the basic solution, $\hat{C}(x,y,z,t)$ and $\hat{p}(x,y,z,t)$, should be calculated and then the final solution will be $C(x,y,z,t) = C^B(z,t) + \hat{C}(x,y,z,t)$ and $p(x,y,z,t) = p^B(z,t) + \hat{p}(x,y,z,t)$.

As usual in linear stability theory, the perturbation in CO_2 concentration is considered as $\hat{C}(x,y,z,t) = \tilde{C}(z,t)e^{iK_1x+iK_2y}$, where the real number $K = \sqrt{K_1^2 + K_2^2}$ is referred to the dimensionless wavenumber. The dimensionless perturbation is expressed as a generalized Fourier series $\tilde{C}(z,t) = \sum_{n=1}^{\infty} v_n(t)\varphi_n(z/2\sqrt{t})$ where $\varphi_n(\xi) = -(H_{2n-1}(\xi)e^{-\xi^2})/(2^{n-1}\pi^{\frac{1}{4}}\sqrt{\Gamma(2n)})$ is the normalized eigenfunctions that $\{\varphi_n(\xi)\}_{n=1}^{\infty}$ form an orthogonal basis for the Hilbert space H, $\Gamma(x)=(n-1)!$ and $H_m(\xi) = (-1)^m e^{\xi^2}(d^m/d\xi^m)e^{-\xi^2}$ are the gamma function and the Hermite polynominals respectively. $v_n(t)$ are the generalized Fourier coefficients.

Properties of $\tilde{C}(z,t)$ will depend on K, the initial perturbations $\tilde{C}(z,t_0)$ at a given initial time t_o, and $F = \sqrt{k_h/k_v}$ where k_h is absolute horizontal permeability. For $t \geq t_0$, the time behaviour of $\theta(t;K,F) = \theta(t) = \int_0^{\infty} \tilde{C}^2(z,t)dz$ is used to evaluate the stability properties of $\tilde{C}(z,t)$. It has been demonstrated that $d\theta(t)/dt > 0$ for $t > t_{ins}(K,F)$, where $t_{ins}(K,F)$ is the minimum time for onset of instability for the given K and F. For given F, the minimum of $t_{ins}(K,F)$ as a function of K in the critical time, $t_c(F)$, and the value of the K for which the critical time is obtained in the critical wavenumber, $K_c(F)$. Wessel-Berg [4] also proposed a different definition of the later time called as time of transition to instability. For practical applications, the second

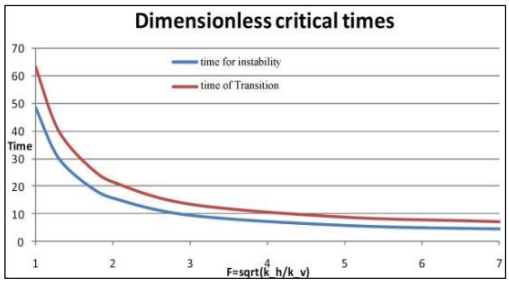

Fig. 1. Dimensionless critical times as a function of F

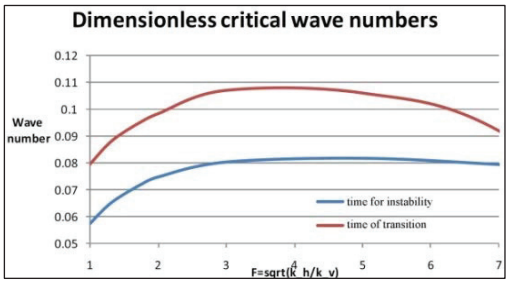

Fig. 2. Dimensionless critical wavenumber as a function of F

definition is probably more appropriate. The critical times $t_c(F)$ and wavenumbers $K_c(F)$ as a function of F are given in Fig. 1 and Fig. 2.

It has been reported [5] that physical critical time for instability and critical wavelength of a perturbation which most easily gives rise to instability are in the forms of:

$$t_c^* = D\left(\frac{\varphi\mu}{\Delta\rho g k_v}\right)^2 t_c(F) \qquad \ldots\ldots\ldots\ldots (1)$$

$$\lambda_c^* = \frac{2\pi L}{K_c(F)} = \left(\frac{2\pi\varphi D\mu}{\Delta\rho g k_v}\right)\left(\frac{1}{K_c(F)}\right) \qquad \ldots\ldots\ldots\ldots(2)$$

3. Simulation analyses

3.1. Simulation models

Eclipse-100 flow simulator (black oil) is used in this study [6]. The simulation models are two-phase flow, two-dimensional and are initialized with a gas cap containing free phase CO_2 on top with aquifer below. Convective mixing results when one introduces a perturbation from the pure diffusion profile which results from CO_2 diffusing into the aquifer below the phase contact.

The simulation models have the porosity of 0.2, diffusion coefficient of 4.00×10^{-10} m^2/s and brine viscosity of 1.0×10^{-3} Pa.s (1 cp). The defined PVT properties of CO_2 and brine cause maximum density difference of brine due to CO_2 dissolution to be 8.25 kg/m^3. The models depths are large enough for occurrence of instability considering their equivalent Rayleigh numbers ($R_a \approx$ 360- 500). The time steps are fine enough to have the capability for capturing of the critical times with high accuracy.

The accurate modeling of convection fingers requires very fine grid block sizes. The critical horizontal wavelength of a perturbation which most easily gives rise to instability can be considered as an indication for appropriate grid size of the model in numerical simulation. A sensitivity analyses on grid block sizes shows that the grid block size with 1/20 of critical wavelength obtained from linear stability analysis (Equation 2) can be a suitable size for simulation of this phenomena. By increasing the grid block size, the initial fingering will not be captured and the onset time for convection is delayed.

3.2. New approach for initializing of the model

For involving of theoretical concepts into simulation model, a wavy perturbation that is consistent with the perturbation in linear stability analysis theory is arranged and introduced into simulation model. For this purpose, every twenty grid blocks in x-direction are allocated to a period of initial perturbation and an equilibrium region is assigned to any of these twenty grid blocks in x-direction. For each equilibrium regions a dissolved CO_2 into brine that varies vertically is defined. These defined properties for the first

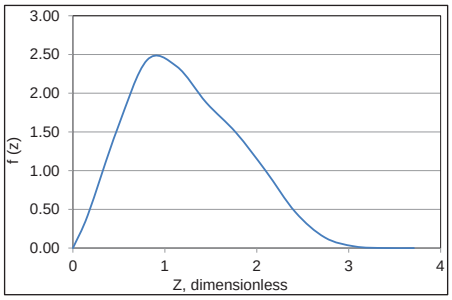

Fig. 3. Variation of f(Z) vs. Z

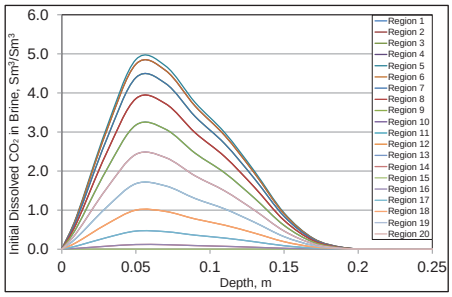

Fig. 4. Variation of dissolved CO_2 into brine with depth

period are repeated for the next ones. The wavy perturbation introduced into the simulation model using the dissolved CO_2 into brine is:

$$Rs_i = f(Z_i)\left[sin\left(\frac{2\pi}{\lambda_c^*} i\Delta x\right) + 1\right] \quad (3)$$

where Rs_i is dissolved CO_2 into brine in grid block i in x-direction, $f(Z_i)$ is the perturbation function for instability that $Z = z/2\sqrt{t}$ and t is dimensionless time before instability, e.g. 40 and $\Delta x = \lambda_c^*/20$.

Similar to perturbation function in linear stability analysis, the required perturbation for instability in the simulation model is defined as:

$$f(Z) = \alpha \sum_{1}^{\infty} \gamma_i \varphi_i(Z) = \alpha[0.69\varphi_1(Z) + 0.64\varphi_2(Z) + 0.23\varphi_3(Z) - 0.16\varphi_4(Z) - 0.07\varphi_5(Z) + 0.10\varphi_6(Z)]$$

where γ_i coefficients are extracted from Fig. 5 in Wessel-Berg work [4] and α is a scaling coefficient such that $0 < f(Z) < [\max(Rs)/2]$.

For a given dimensionless depth, f(Z) is related only to α and t and consequently the defined wavy perturbation is related to α, t, critical wavelength and grid size. Fig. 3 shows the variation of f(Z) vs. Z for a case with t= 60 and α= -10 and Fig. 4 shows the variations of the dissolved CO_2 into brine with depth for all twenty regions for an isotropic case with t= 60 and α= -10 and permeability of 2.47×10^{-13} m^2 (250 md). It can be seen that region 5 has the most dissolved CO_2 into brine at all depths.

This approach for initializing of the brine aquifer models is used in this work and at the first step the optimum values of t and α should be determined. Some sensitivity analyses on t (t= 20, 30, 40, 50, 60 and 70) and α (α= -0.01, -0.1, -1, -10, -30 and -50) are performed in isotropic brine aquifer models with critical wavenumber of 0.0574 (from Fig. 2), permeabilities of 250 and 25000 md and equivalent Rayleigh number of 499.75.

Fig. 5 shows the effect of t on the amount of dissolved CO_2 into brine for models with permeability of 250 md and α= -1 and compares them with the results of the model which the instability is triggered by numerical round off errors. It can be seen that dissolution mechanism in all models is started as diffusion and after onset time for convection, the dissolution rate is increased. It is obvious that the critical times are smaller in the cases which have been initialized with the new approach. Also increasing the t causes negligible decreases in critical time and increase in the total dissolved CO_2 into brine. As it is difficult to distinguish the critical times from this figure, the behaviour of θ(t) and the sign of dθ(t)/dt are considered for exact determination of critical times. The time at minimum of θ(t) or the time when dθ(t)/dt>0 is considered as critical time. For calculation of θ(t), the calculated Rs in region 5 of the model (because of the highest Rs values) is exported for all depths and all times before and after onset time for convection. After scaling these exported Rs values to dimensionless Rs and using $Rs_{d5}(z,t) = C_5(z,t) = erfc\left(z/2\sqrt{t}\right) + \tilde{C}(z,t)$, the dimensionless perturbation, $\tilde{C}(z,t)$, can be calculated and using $\theta(t) = \int_0^{\infty} \tilde{C}^2(z,t)dz$, the θ(t) and

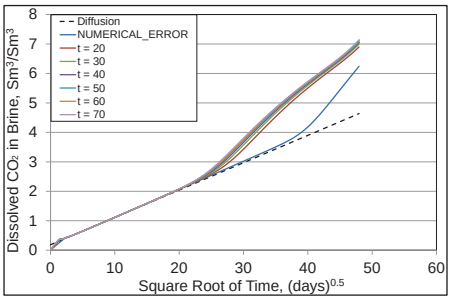

Fig. 5. Effect of t on the amount of dissolved CO_2 into brine

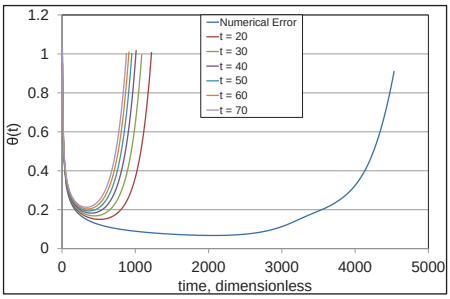

Fig. 6. Variation of θ(t) for different values of t

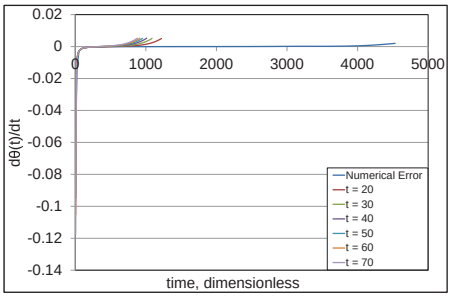

Fig. 7. Variation of dθ(t)/dt for different values of t

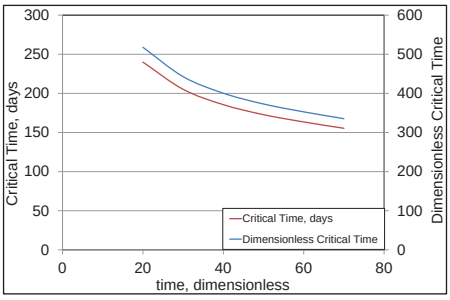

Fig. 8. Effects of t on critical time

dθ(t)/dt can be calculated. Fig. 6 and Fig. 7 indicate variation of θ(t) and dθ(t)/dt for different values of t in the cases with permeability of 250 md and α= -1. From Fig. 6 it can be seen that there is a shift from right to left by increasing the t and critical time is decreased by increasing the t. While in the model which the instability is triggered by numerical round off errors, this time is too late in comparison to the models that are initialized with the new approach. Fig.7 shows similar results and demonstrates that all models start with diffusion and negative values of dθ(t)/dt and at critical time that is decreased by increasing t, the sign of dθ(t)/dt is changed. Fig. 8 is a conclusion for the effects of t on critical time in this sensitivity analysis and it shows that increasing of t from 20 to 70 causes decrease of dimensionless critical time for convection from 518 to 335 while the theoretical critical times (from Fig. 1) are 48.49 and 63.12 as time for instability and time of transition respectively. Considering definition of t in Equation 3 that is the dimensionless time before instability and the results of this analysis, it seems that t= 60 can be the optimum value for this approach in this case.

Fig. 9 shows the effect of α on the amount of dissolved CO_2 into brine for models with permeability of 250 md and t=40. It can be seen that α has considerable effects on convection process in comparison to t and increasing the absolute value of α causes a significant decrease of critical time and increase of the total amount of dissolved CO_2 into brine in comparison to the results of the model which the instability is triggered by numerical round off errors. Also it seems that for very high absolute value of α like 30 and 50, the diffusion process before critical time is misleading. Hence the selection of the optimum value for α is important. Fig. 10 and Fig. 11 show variation of θ(t) and dθ(t)/dt for this analysis and it is concluded that increasing the absolute value of α causes increasing and shifting of θ(t) from right to left and subsequently decreasing of critical time. While the critical time in the model with numerical errors is much later than those predicted in the models with new initializing approach. Fig. 12 shows the effects of α on critical time and it demonstrates that increasing the absolute value of α from 0.01 to 50 causes decrease of dimensionless critical time for convection from 490 to 52. Also this variation is severe for

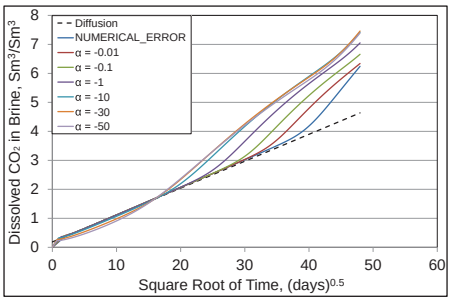

Fig. 9. Effect of α on the amount of dissolved CO_2 into brine

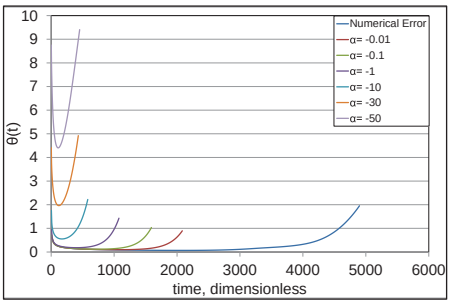

Fig. 10. Variation of θ(t) for different values of α

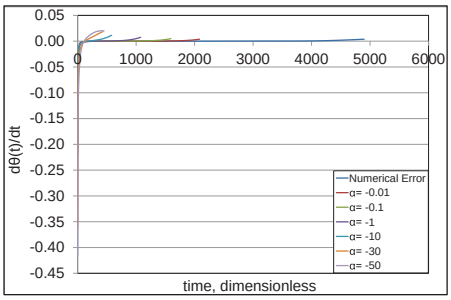

Fig. 11. Variation of dθ(t)/dt for different values of α

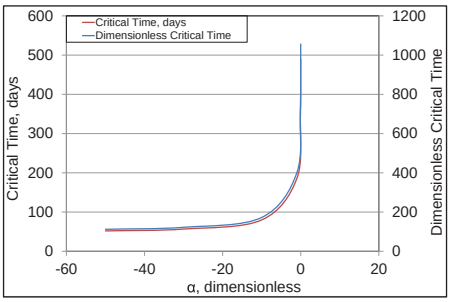

Fig. 12. Effects of α on critical time

absolute values below 10. Considering the confusing behaviour of diffusion process in the cases with α of -30 and -50, α =-10 is considered as the optimum value for this methodology in this case.

For model with permeability of 25000 md, the same results were concluded and eventually, the optimum values for t and α are determined as 60 and -10 respectively.

3.3. Isotropic models

Permeability is the most important parameter for onset time for convection in an isotropic brine aquifer with F=1. In this section the new approach is used for initializing of the models with different permeabilities to see the effect of permeability on critical time. For this purpose, the models with permeabilities of 250, 500, 1000, 5000, 10000 and 25000 md and equivalent Rayleigh number of 499.75 are considered for study. The critical wavenumber of the system is 0.0574 (Fig. 2).

Fig. 13 show variations of θ(t) for the isotropic cases with different permeabilities that were initialized with new approach. It can be seen that permeability has no effect on θ(t) and consequently the dimensionless critical time. This is equivalent to theoretical results that show the dimensionless critical time is only a function of F (Fig. 1). While it can be seen in Fig. 14 that this result cannot be concluded for the isotropic cases which instability is triggered by numerical round off errors. Fig. 15 compares the dimensionless critical times calculated from different methodology. It shows that using the new approach for initializing of the model can yield the most acceptable results in comparison to those which instability is activated by numerical round off errors. The dimensionless critical time in cases that were initialized with new approach is 144.58, while it is in the range of 2071 and 3992 for cases with different permeabilities which instability is started by numerical round off errors. Also it should be considered that the theoretical critical time are 48.49 and 63.12 as time for instability and time of transition respectively (Fig. 1).

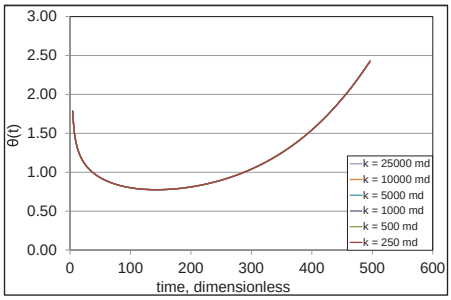

Fig. 13. Variation of θ(t) for different values of k; instability by new initializing approach

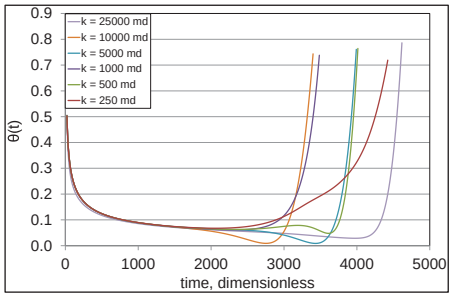

Fig. 14. Variation of θ(t) for different values of k; instability by numerical round of errors

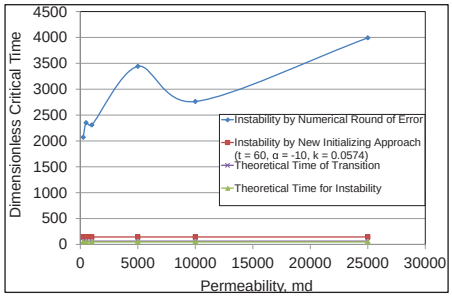

Fig. 15. Dimensionless critical times vs. k with different methodologies

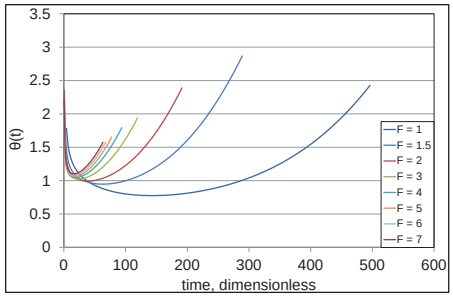

Fig. 16. Variation of θ(t) for different values of F; instability by new initializing approach

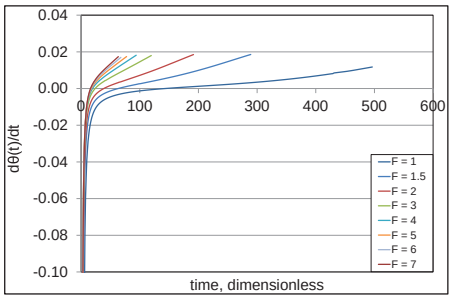

Fig. 17. Variation of dθ(t)/dt for different values of F; instability by new initializing approach

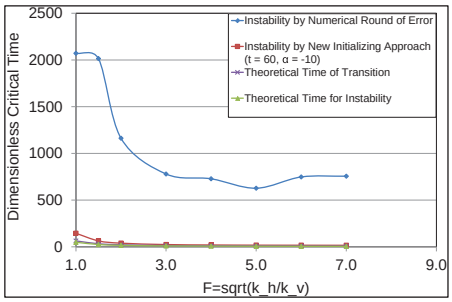

Fig. 18. Dimensionless critical times vs. F with different methodologies

3.4. Anisotropic models

For testing of the new initializing approach in anisotropic systems, 48 cases with horizontal permeabilities of 250, 500, 1000, 5000, 10000 and 25000 md and F of 1, 1.5, 2, 3, 4, 5, 6 and 7 with equivalent Rayleigh numbers of 364 to 479.75 are considered. For each value of F, the dimensionless critical wavenumber are read from Fig. 2 and critical wavelengths are calculated.

Fig. 16 and Fig. 17 show variation of θ(t) and dθ(t)/dt for the anisotropic cases with different F that were initialized with new initializing approach. This behaviour exists for all permeability values and as it was investigated in previous section, the permeability has no effect on θ(t), dθ(t)/dt and the dimensionless

critical time. These two figures show that by increasing the F, the curve of θ(t) is shifted to the left and consequently the dimensionless critical time is decreased. Also the change in sign of dθ(t)/dt to positive happens earlier in the cases with higher F. These results are shown in Fig. 18 that compares the results of different methodologies for calculation of dimensionless critical time. It can be seen that the dimensionless critical times in the cases which instability is triggered by numerical round off errors are far from values calculated from theoretical methods, while those ones in the cases that were initialized with the new approach has acceptable values

4. Conclusions

In this study, a new approach for initializing the numerical models was developed that causes more accurate predictions of critical times in isotropic and anisotropic brine aquifer models. For using of the new initializing approach, the optimum values for two parameters of t and α should be determined. Increasing of the t causes negligible decreases in critical time while increasing the absolute value of α causes a significant decrease of critical time. Also the behaviour of θ(t) and dθ(t)/dt was considered as an exact method for determination of critical times. Permeability has no effect on behaviour of θ(t) and dθ(t)/dt and subsequently the dimensionless critical time. By increasing the F, the curve of θ(t) is shifted to the left and consequently the dimensionless critical time for convection is decreased.

Acknowledgements

This publication has been produced with support from the BIGCCS Centre, performed under the Norwegian research program Centres for Environment-friendly Energy Research (FME). The authors acknowledge the following partners for their contributions: Aker Solutions, ConocoPhilips, Det Norske Veritas AS, Gassco AS, Hydro Aluminium AS, Shell Technology Norway AS, Statkraft Development AS, Statoil Petroleum AS, TOTAL E&P Norge AS, GDF SUEZ E&P Norge AS and the Research Council of Norway (193816/S60).

References

[1] Lindeberg E., Wessel-Berg D. Vertical convection in an aquifer column under a gas cap of CO_2. Energy Convers Manage (1996), 38 (Suppl.): 229–234.

[2] Lindeberg E, Wessel-Berg D. Upscaling studies of diffusion induced convection in homogeneous and heterogeneous aquifers. Energy Procedia 4 (2011), 3927–3934.

[3] Taheri A, Wessel-Berg D, Torsæter O, Soroush M. The Effects of Anisotropy and Heterogeneity on CO_2 Dissolution in Deep Saline Aquifers. Paper CMTC 151345, presented at the Carbon Management Technology Conference held in Orlando, Florida, USA, 7–9 February 2012.

[4] Wessel-Berg D. The Gravitational Instability of a Diffusive Boundary Layer; towards a Theoretical Minimum for Time of Onset of Convection. presented at the 13th European Conference on the Mathematics of Oil Recovery, 10-13 September 2012, Biarritz, France.

[5] Vad´asz P. Emerging Topics in Heat and Mass Transfer in Porous Media. Springer Science+, Business Media B.V., Berlin, 2008.

[6] Schlumberger. Eclipse- 100 Reservoir Simulator. V- 2011.1, 2011.